

Influence of Hydrogen on Multiple-Electrode (Vacuum) Gap Characteristics

Sol Schneider, Anthony J. Buffa, and John E. Creedon

Citation: *Journal of Applied Physics* **40**, 424 (1969); doi: 10.1063/1.1657077

View online: <http://dx.doi.org/10.1063/1.1657077>

View Table of Contents: <http://scitation.aip.org/content/aip/journal/jap/40/1?ver=pdfcov>

Published by the AIP Publishing

Articles you may be interested in

[Using multiple-electrode impedance measurements to monitor cryosurgery](#)

Med. Phys. **29**, 2806 (2002); 10.1118/1.1521721

[Results for two children using a multiple-electrode intracochlear implant](#)

J. Acoust. Soc. Am. **86**, 2088 (1989); 10.1121/1.398468

[A wearable multiple-electrode electrotactile speech processor for the profoundly deaf](#)

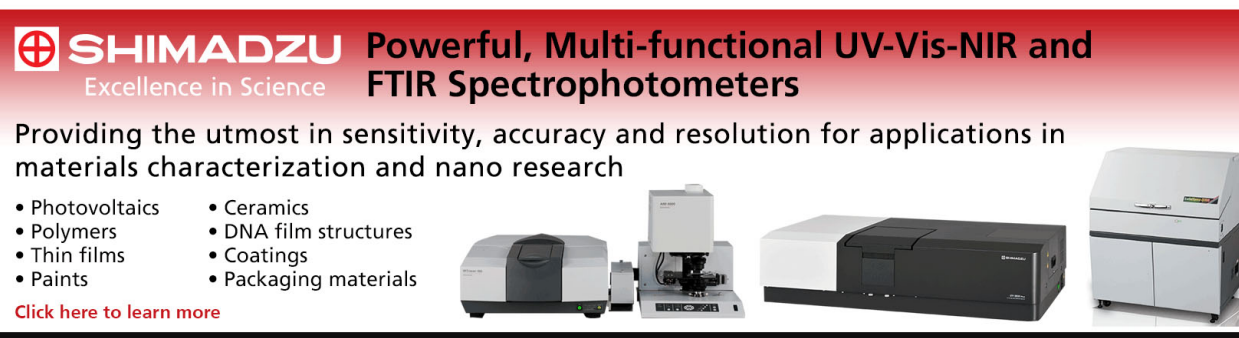
J. Acoust. Soc. Am. **77**, 1619 (1985); 10.1121/1.392009

[Speech processing for a multiple-electrode cochlear implant hearing prosthesis](#)

J. Acoust. Soc. Am. **68**, 1897 (1980); 10.1121/1.385184

[Design criteria of a multiple-electrode cochlear implant hearing prosthesis](#)

J. Acoust. Soc. Am. **63**, 631 (1978); 10.1121/1.2033198

This is a promotional banner for Shimadzu spectrophotometers. It features the Shimadzu logo (a red circle with a white cross) and the text 'SHIMADZU Excellence in Science' on the left. To the right, the headline reads 'Powerful, Multi-functional UV-Vis-NIR and FTIR Spectrophotometers'. Below this, a sub-headline states 'Providing the utmost in sensitivity, accuracy and resolution for applications in materials characterization and nano research'. A bulleted list of applications is provided: Photovoltaics, Polymers, Thin films, Paints, Ceramics, DNA film structures, Coatings, and Packaging materials. A red link 'Click here to learn more' is positioned below the list. On the right side of the banner, four different models of Shimadzu spectrophotometers are shown, ranging from compact benchtop units to larger floor-standing models.

SHIMADZU Excellence in Science **Powerful, Multi-functional UV-Vis-NIR and FTIR Spectrophotometers**

Providing the utmost in sensitivity, accuracy and resolution for applications in materials characterization and nano research

- Photovoltaics
- Polymers
- Thin films
- Paints
- Ceramics
- DNA film structures
- Coatings
- Packaging materials

[Click here to learn more](#)

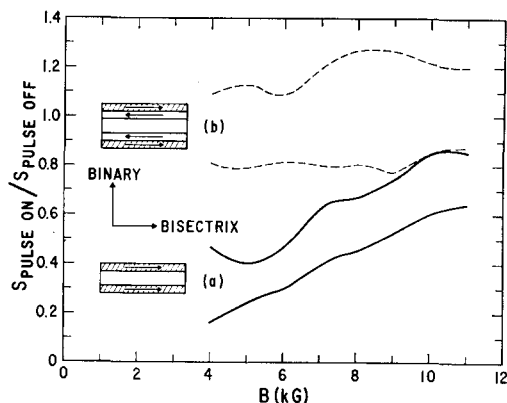


FIG. 2. The ratio of the helicon amplitude with current pulse on to the helicon amplitude with the current pulse off as a function of magnetic field for (a) solid curves, metal-Bi(Te)-metal sandwich and (b) dashed curves, metal-Bi(Te)-Be(Te)-Bi(Te)-metal sandwich. The data were taken at 10 MHz and 4.2°K with a pulse current of ~ 450 A and the crystalline axes oriented as shown. The electron density of the Bi(Te) bars was $6.7 \times 10^{17} \text{ cm}^{-3}$. The relative current directions in the bars are indicated in the figure. In both cases the upper curve was obtained when the electrons were drifted in the direction of wave propagation.

difference was the use of Fabry-Perot geometry. Initially we used the traveling-wave technique; however, due to low-signal levels and great difficulty in eliminating reflections at these low frequencies (probably due to the high $\omega_c \tau$ values reached) the Fabry-Perot geometry was adopted. It has been shown that this geometry is convenient for studying helicon amplification and that the Fabry-Perot resonance condition is not changed by carrier drift.¹¹ The principal problem with this configuration is the need to compare results from structures of different lengths in order to demonstrate amplification.

The fact that changes in attenuation of the wave propagating through the sandwich structure are partially due to magnetoresistance effects is demonstrated by the curves (a) in Fig. 2 which were obtained for a metal-Bi(Te)-metal sandwich. Although the magnetic fields due to currents through the metal bars tend to cancel, the inhomogeneous magnetic field within a 0.1 cm thick center bar has a maximum value of ~ 570 G for a pulse current of 450 A, which was the maximum used in the experiment. If the doping of the center bar were completely uniform, the dependence on current direction exhibited by curves (a) should not be present. However, the magnetoresistance of pure Bi is known to be highly anisotropic,¹² and this fact in combination with a slight nonuniformity in doping probably accounts for the observed dependence on current direction in the case of Bi(Te). The duty cycle of the pulse current was varied to make certain that there were no effects due to sample heating. Most of the sandwich structure measurements were made with the configuration used to obtain curves (b) in Fig. 2. The outer metal bars were included in the pulse circuit in order to minimize magnetoresistance effects. The pulse magnetic field in the center bar was reduced to the point that it did not affect propagation in this bar. This was confirmed by using a metal-metal-Bi(Te)-metal-metal structure with the current directions the same as in Fig. 2(b). It was not possible to separate magnetoresistance effects in the outer Bi(Te) bars from effects due to instabilities.

Our experimental results for various sandwich structures can be summarized as follows. The structures were typically 1.0–1.5 cm long and 0.2 cm wide. The center bar was 0.1–0.2 cm thick, and the outer bars were 0.025–0.050 cm thick. The ratio of the dielectric constant in the center bar to that in the outer bars ranged from 1.0–1.4. In some of the structures investigated, the condition $v_D > v_\phi$ was reached. In all cases, the wave was attenuated less when the carriers were drifted in the direction of wave propagation; however, the increase in signal level ob-

served in the case of Fig. 2(b) was not always observed. In fact, an increase in attenuation ($\sim \times 2$) was observed for both directions of drift in the structures for which $v_D > v_\phi$. These results indicate that the observed effects are due to a combination of magnetoresistive effects and the bulk instability described by Baraff.² Any effects due to a surface wave instability in the sandwiches with a dielectric mismatch would have had the opposite dependence on the direction of electron drift than was actually observed. The largest increase in amplitude which was observed was by a factor of 1.4. This is in contrast to the increase in amplitude of 5.5 reported by Nanney *et al.*³ They did not report observing any magnetoresistance effects (perhaps because $\omega_c \tau$ saturates).

We conclude that although it is possible to achieve relatively large $\omega_c \tau$ in Bi(Te) any effects due to the surface wave instability are obscured by magnetoresistance effects and a competing bulk instability. The presence of these other effects and our inability to attain the optimum experimental conditions prevent us from drawing any conclusions concerning the validity of the surface-wave instability theory. It should be noted, however, that all of the materials presently available which potentially could be used to study the surface-wave instability either exhibit $\omega_c \tau$ saturation or pronounced magnetoresistance effects.

The author wishes to thank G. A. Antcliffe, R. T. Bate, and D. L. Carter for helpful discussions about this experiment, G. R. Cronin and D. Thompson for providing the Bi(Te) crystals, and C. A. Collins for his help with the experimental work.

¹ G. A. Baraff and S. J. Buchsbaum, *Appl. Phys. Letters* **6**, 219 (1965); *Phys. Rev.* **144**, 266 (1966).

² G. A. Baraff, *J. Phys. Chem. Solid* **28**, 1037 (1967).

³ S. J. Buchsbaum, *Proceedings of the Symposium on Plasma Effects in Solids, Paris, 1964* (Dunod Cie., Paris, 1965), pp. 3–18.

⁴ J. Bok and P. Nozleres, *J. Phys. Chem. Solids* **24**, 709 (1963); A. Bers and A. L. McWhorter, *Phys. Rev. Letters* **15**, 755 (1965).

⁵ R. N. Wallace and G. A. Baraff, *J. Appl. Phys.* **37**, 2937 (1966).

⁶ C. A. Nanney, A. Libchaber, and J. P. Garino, *Appl. Phys. Letters* **9**, 395 (1966).

⁷ W. R. Wiseman and E. J. Davies, *J. Appl. Phys.* **38**, 3940 (1967).

⁸ C. Herring, *J. Appl. Phys.* **31**, 1939 (1960); R. T. Bate, *Semiconductors and Semimetals*, R. K. Willardson and A. C. Beer, Eds. (Academic Press Inc., New York, 1968), Vol. 4, p. 459.

⁹ B. H. Schultz and J. M. Noothoven van Goor, *Philips Res. Rept.* **19**, 103 (1964).

¹⁰ G. A. Antcliffe (private communication).

¹¹ W. R. Wiseman, *Phys. Letters* **28A**, 57 (1968).

¹² S. Mase, S. von Molnar, and A. W. Lawson, *Phys. Rev.* **127**, 1030 (1962).

Influence of Hydrogen on Multiple-Electrode (Vacuum) Gap Characteristics

SOL SCHNEIDER, ANTHONY J. BUFFA, AND JOHN E. CREEDON

Electron Tubes Division, Electronic Components Laboratory, U.S. Army Electronics Command, Fort Monmouth, New Jersey 07703

(Received 29 July 1968; in final form 21 August 1968)

The influence of a low pressure of hydrogen on the voltage hold-off and breakdown characteristics of a multiple-electrode triggered vacuum gap has been investigated using the structure shown in Fig. 1. The tube is designed for 300 kV operation. The tube characteristics were studied under vacuum and at several hydrogen fill pressures at voltages from 10–300 kV. A dc voltage divider of 540 M Ω was connected to the tube to provide equal voltage division across the electrode during the capacitor charging period. The capacitor bank was 0.125 μF and had a 105 Ω current-limiting resistor. Trigger current, anode current, and voltage were monitored. The anode current and voltage waveforms were essentially similar in shape, since the tube basically behaved like a varying resistor.

Figure 2 shows the results from 10–300 kV for the tube when operated in the high-vacuum mode. The bottom curve shows

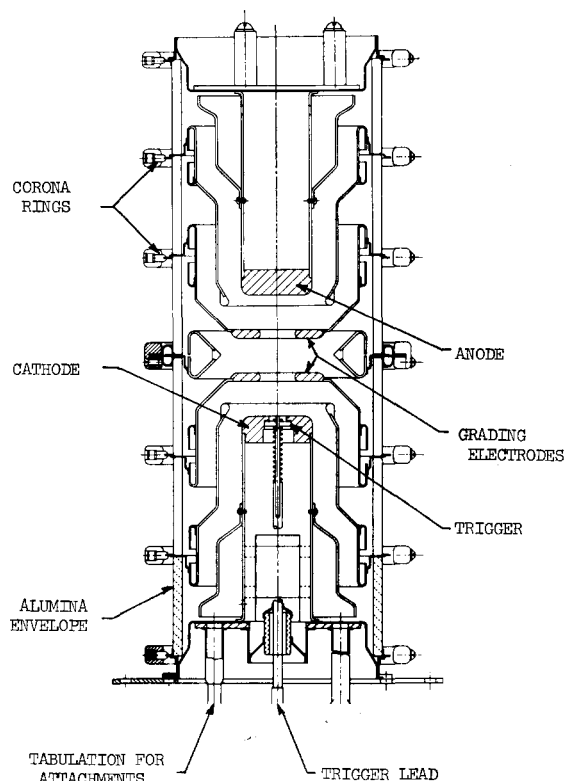


FIG. 1. Schematic drawing of the tube structure. It is of ceramic-metal construction with the anode, grading electrodes, and cathode made of zone-refined copper. Electrode separations are 1 in., and the total discharge-path length is 3.5 in. A zirconium-hydride plasmoid-type trigger is inserted in the cathode. A titanium-hydride reservoir and an ion pump are attached.

the delay from initiation of the trigger current to initiation of the anode current, which is about $0.75 \mu\text{sec}$ and is independent of anode voltage. The top curve shows the time to reach full anode conduction from initiation of the trigger pulse. This time is shown since voltage waveforms indicated that this coincides with complete establishment of the arc. Note that at 10 kV, it is $1.6 \mu\text{sec}$ and rises to $3.7 \mu\text{sec}$ at 50 kV. It remains essentially flat to 200 kV, after which it falls gradually. Apparently over 200 kV, the anode voltage assists breakdown. The middle curve shows the current risetime, from 0-100% after initiation of anode current. The current risetime is approximately $3.0 \mu\text{sec}$ over most of the voltage range.

Figure 3 shows the results obtained with 15 mTorr of hydrogen added to the tube. The anode delay time has changed slightly. It is approximately 50 nsec less than the vacuum case. The big difference is in the time to reach peak anode current (the top curve). At 7.0 kV, it is $1 \mu\text{sec}$ and rises to approximately $2.4 \mu\text{sec}$

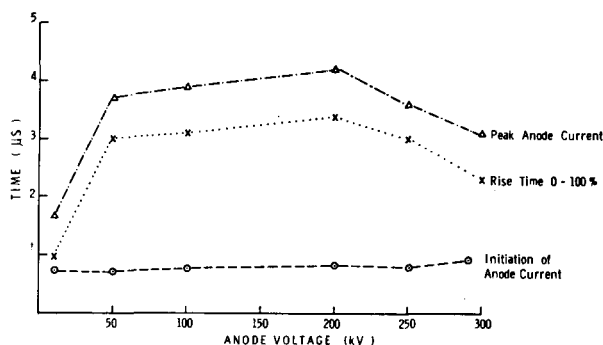


FIG. 2. Results obtained under vacuum conditions.

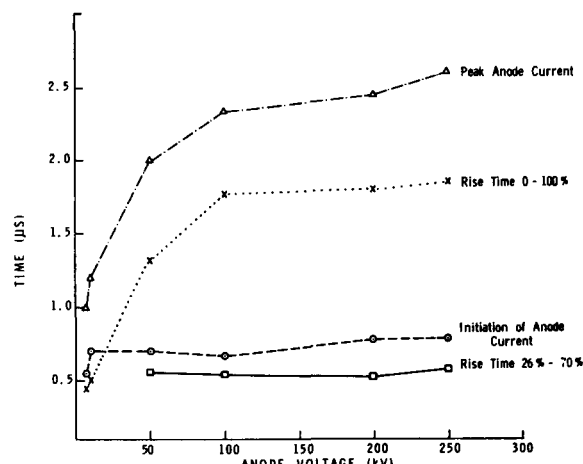


FIG. 3. Results obtained with 15 mTorr of hydrogen.

at 100 kV and remains relatively constant thereafter. Subtracting the anode delay time shows the risetime from 0%-100% is a maximum of $1.8 \mu\text{sec}$ for any voltage. The bottom curve shows the time constant for current rise from the 26%-70% points. It is approximately $0.55 \mu\text{sec}$ and is completely independent of voltage. The characteristics shown were also independent of gas pressure over the range of 7-25 mTorr.

With respect to voltage hold-off, under vacuum conditions, frequent spurious breakdowns occurred at 300 kV. The addition of hydrogen gave reliable hold-off at 320 kV at hydrogen pressure up to 50 mTorr. Over 50 mTorr, the voltage hold-off characteristics deteriorated. This result is consistent with recent observations by Cooke¹ on the influence of a nitrogen atmosphere on voltage-breakdown properties of a single gap.

¹ C. M. Cooke, in *Proc. 2nd Intern. Symp. on Insulation of High Voltages in Vacuum* (1966), p. 181.

Reaction-Process Dependence of Barrier Height between Tungsten Silicide and *n*-Type Silicon

YOKICHI ITOH AND NORIKAZU HASHIMOTO

Central Research Laboratory, Hitachi Ltd., Kokubunji, Tokyo, Japan

(Received 3 April 1968; in final form 3 October 1968)

Recently, thin metal films whose eutectic temperatures with silicon were more than 1000°C were chemically deposited on silicon substrates using the process of hydrogen reduction or thermal decomposition of metal halides.¹⁻³ In the case of hydrogen reduction of tungsten hexachloride, we have reported⁴ that the barrier height of about 0.86 eV was observed from the photoelectric

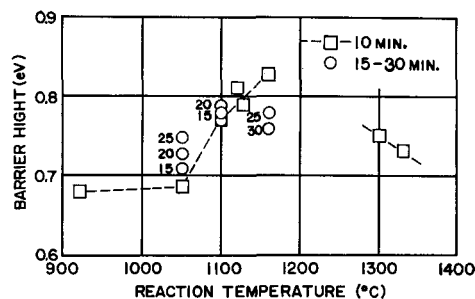


FIG. 1. Reaction-temperature dependence of tungsten silicide and *n*-type silicon barrier height is shown. Squares and circles stand for different reaction times, from which reaction-time dependence of the barrier heights is observed.